Mineralogy and trace element chemistry of the Siliceous Earth of Barmer basin, Rajasthan: Evidence for a volcanic origin

M S Sisodia[1], U K Singh[1], G Lashkari[1], P N Shukla[2], A D Shukla[2] and N Bhandari[2*]

[1]*Department of Geology, JNV University, Jodhpur 342 005, India.*
[2]*Physical Research Laboratory, Navrangpura, Ahmedabad 380 009, India.*
[*]*e-mail: bhandari@prl.ernet.in*

We report the presence of a 3–5 cm thick loose fragmental layer in the Siliceous Earth at Matti ka Gol in the Barmer basin of Rajasthan. Petrographic, chemical and mineralogical study reveals the presence of abundant volcanic debris such as glass shards, agglutinates, hollow spheroids, kinked biotites, feldspars showing oscillatory zoning, olivines, ilmenite and native iron. The presence of similar particles in the whole section suggests that the Siliceous Earth is a volcanic ash. Stratigraphic correlation, palynological and microvertebrate data suggest that the Siliceous Earth may have deposited over a short span of time during the Upper Cretaceous to Lower Palaeocene. In view of the possibility that this section may contain K/T impact debris, we looked for grains having impact signatures. Some patches of the Siliceous Earth of Bariyara show the presence of Ni-rich ($> 0.5\%$) vesicular glasses, sanidine spherules, magnesioferrite crystals, soot, etc., but because of their low abundance, it is not possible to establish if they are volcanic, micrometeorite ablation products or a part of the K/T impact ejecta.

1. Introduction

The Barmer basin of Rajasthan, India has a patchy, thin stratum of opaline silica sediment called 'Siliceous Earth'. It occurs as isolated surface deposits of 1 to 3 m thickness between latitudes N26°20′ and 26°35′ and longitudes E71°00′ and 71°25′, covering an area of about 1600 km^2 (figure 1). It is soft, porous, homogeneous, light-weight (density ~ 0.9 g/cc) and forms a separate sedimentary unit in the Barmer basin. Its major composition varies in a wide range. It mainly consists of silica (75 to 91%) and alumina (3 to 11%) with minor quantities of iron (0.6 to 2.1%), magnesium ($\sim$ 0.4 to 1.4%) (Bhargava and Pitliya 1984; Nahar *et al* 1997). No serious attempt has so far been made to find out its origin. To understand the process of its formation, we have carried out a detailed chemical analysis of samples collected from two exposed sections of the Siliceous Earth. Here we discuss these results in the light of stratigraphic, geological and geochronological framework.

2. Geology of the area

The Barmer basin in western Rajasthan is a narrow north–south trending graben comprising sediments of Middle Jurassic to Lower Eocene age (Das Gupta 1975; Pareek 1981; Mishra *et al* 1993). It originated due to the break up of Indian craton in the latest Cretaceous–early Palaeocene that led to the formation of the Cambay rift and the constituent basins (Sisodia and Singh 2000). Sisodia and Singh (2000) have discussed the stratigraphy of Barmer basin and classified its sediments into three categories *viz.*, Pre-rift, Syn-rift and Post-rift. The lithostratigraphy of Barmer basin is given in figure 2.

Keywords. Barmer basin; Siliceous Earth; volcanic ash; micrometeorites; Cretaceous/Tertiary boundary.

J. Earth Syst. Sci. **114**, No. 2, April 2005, pp. 111–124

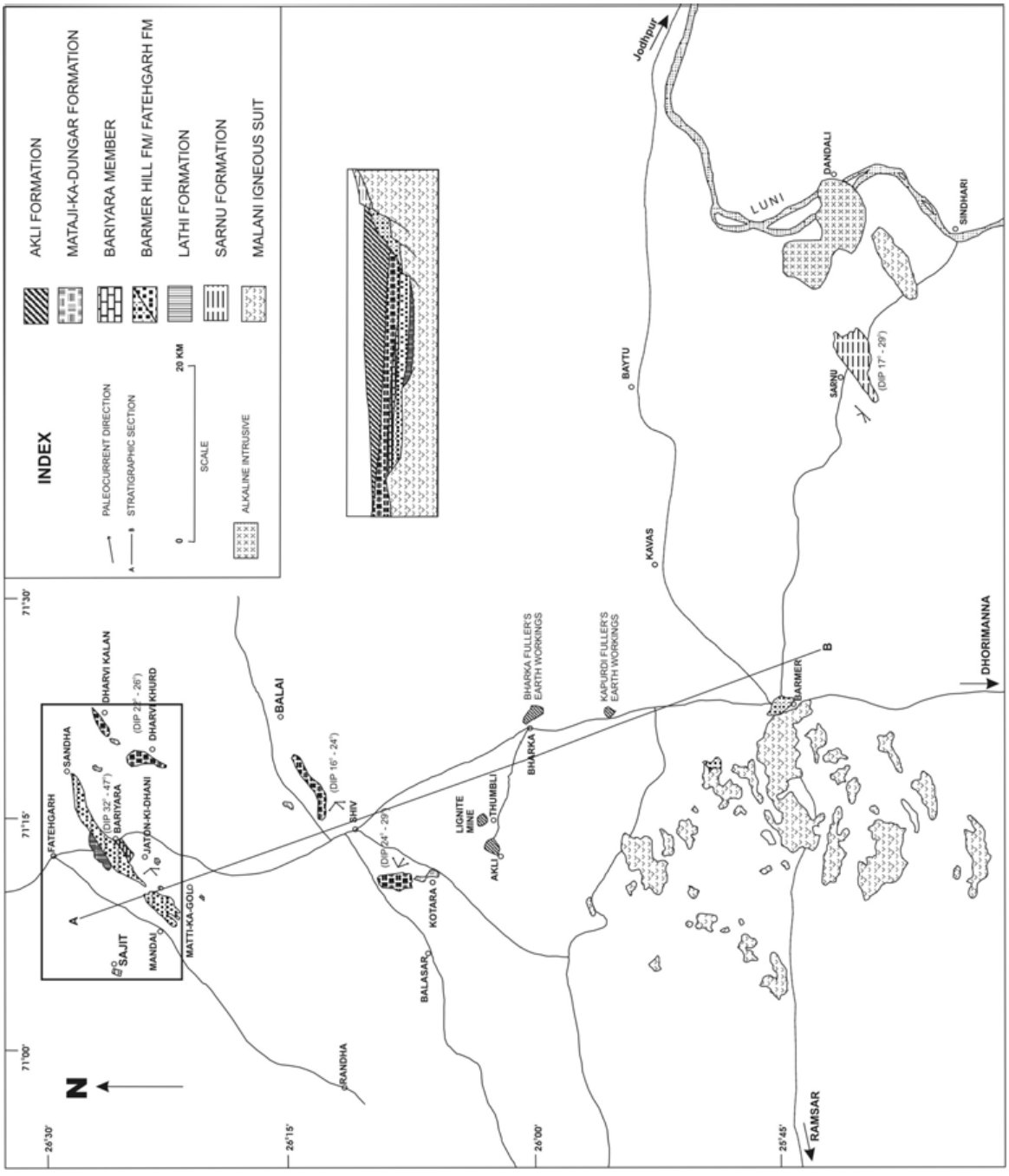

Figure 1. Geological map of Barmer basin, western Rajasthan showing the occurrence of Siliceous Earth near Fatehgarh and igneous rocks in the surrounding area, after Sisodia and Singh (2000).

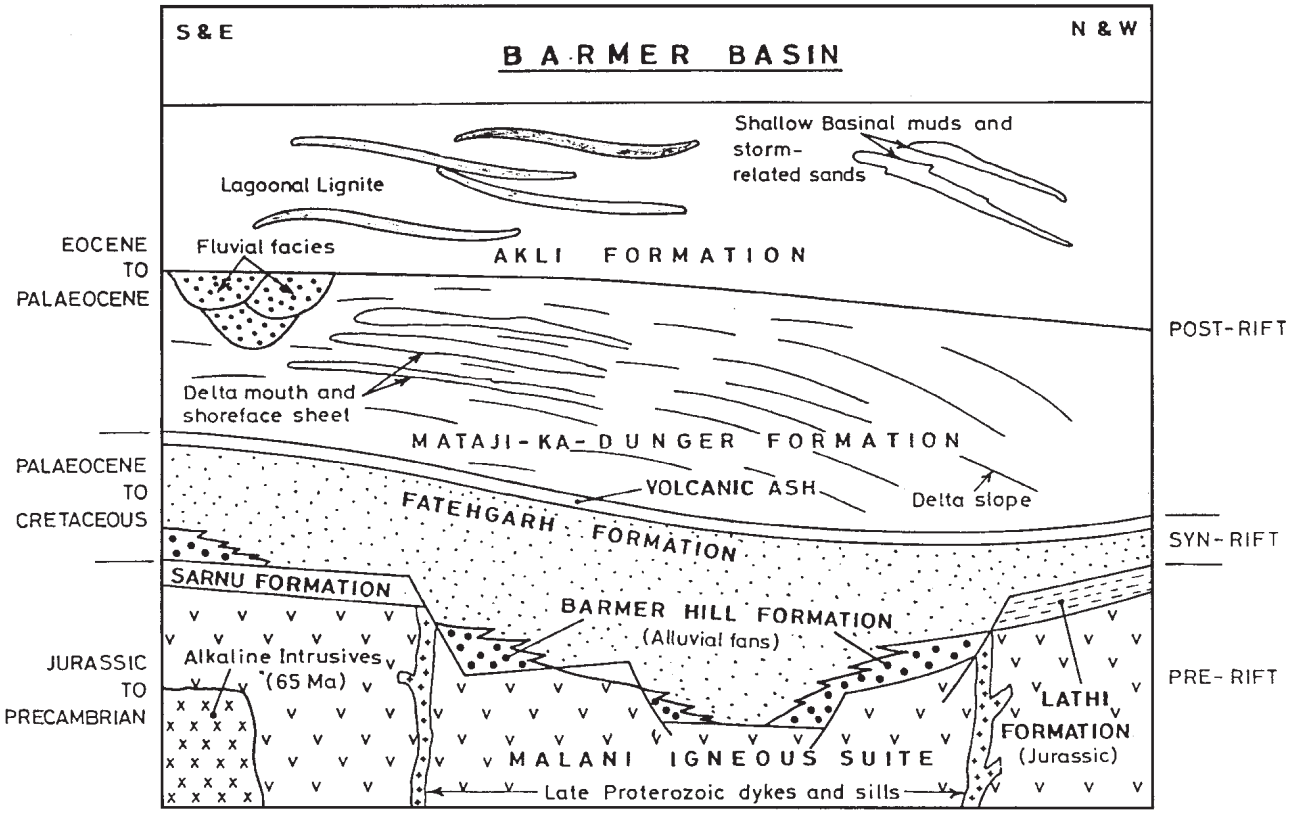

Figure 2. Lithostratigraphy of the Barmer basin, after Sisodia and Singh (2000).

The Pre-rift sediments constitute siliceous Randha Formation, calcareous Birmania Formation; both Lower Palaeozoic in age and Lathi Formation of Liassic age. These sediments are deposited on a Late Proterozoic basement of Malani Igneous Suite.

The Syn-rift formations include Barmer Formation and Fatehgarh Formation. Barmer Formation comprises poorly cemented sandstones and intraformational conglomerate and represents alluvial fan environment. Fatehgarh Formation is mixed sand, mud and phosphorite formation deposited on an intertidal flat environment. It is highly fossiliferous; the phosphorite in this formation is correlated with global Cretaceous upwelling.

The Post-rift sediments deposited as a thickening and coarsening-upward claystone–siltstone–sandstone cycles. They include Akli Formation and Kapurdi Formation. They are of Palaeocene to Eocene age. Overlying Akli and Kapurdi Formations is a grit and gravel bed of Miocene age.

2.1 *Sample details*

We collected several samples of Siliceous Earth from many sections, including a vertical profile from the section at Matti ka Gol (N26°32′: E71°21′) (figure 3) and Bariyara, about 6 km NNE from Matti ka Gol. Their stratigraphic position in the section, together with an abundance of some elements are listed in table 1. The section at Matti ka Gol has three limonitic bands (MG4, MG2 and MG3), each about a centimetre thick. In addition, we found that in the homogenous, uniform bed of the Siliceous Earth at Matti ka Gol lies a 3–5 cm thick layer characterized by its loose fragmental nature. This layer is patchy but traceable in other deposits also e.g., at Bariyara, where it occurs as a < 1 cm thick layer.

3. Experimental procedure

Microscopic examination revealed the presence of some exotic particles that are described in the next section. Some major and trace elements, including lithophile elements (Na, K, Ba, Hf, Sc, Cs, Zr) and nine rare earth elements (La, Ce, Nd, Sm, Eu, Gd, Tb, Yb, Lu), Siderophile elements (Fe, Cr, Co, etc.) and some chalcophile elements (Sb and Zn) were measured by neutron activation (INAA) method. Typically about 150 mg of the samples were irradiated to a fluence of $\sim 10^{18}$ neutrons in the CIRUS reactor at Bhabha Atomic Research Centre, Bombay followed by sequential gamma ray spectrometry after different intervals of time using

Figure 3. Open face of Siliceous Earth quarry at Matti ka Gol.

high purity Germanium detectors. Columbia River basalt (BCR-1), Allende meteorite and several rock powders e.g., W2 and G2 were used as reference standards. Ni could not be measured by neutron activation because of high interference from Eu and hence Ni, as also Fe, Mg, Al, etc., were measured by ICPAES method. Typical errors of counting (1σ) of various elements are shown in table 1. To this must be added other errors of measurement and reproducibility of about 5% in each case.

U and Th chain nuclides (^{234}Th, ^{226}Ra, ^{214}Bi, ^{210}Pb and ^{208}Tl) were measured by gamma ray spectrometry. The gamma ray energies of nuclides based on which the concentrations have been calculated are listed in table 1. To ensure identical absorption factors, particularly for the low energy radionuclides where self-absorption is significant, roughly equal amounts of samples were counted in identical counting geometry. Low background, high sensitivity hyper-pure germanium and low energy planar detectors located in 12-cm thick lead shield were used for this purpose. Basalt standard #107 (U = 5.69 ppm, Th = 14.50 ppm, K = 2.63%), known to have all the decay chain nuclides in equilibrium, was used for calculating the concentration of U and Th daughter nuclides and K in the samples. In order to ensure that the equilibrium of daughter nuclides with ^{226}Ra is not disturbed due to the escape of radon, the nuclides were allowed to grow to the saturation level by keeping the samples sealed for two weeks in a plastic container.

4. Results

Microscopic examination of the fragmental layer reveals the presence of glass shards, agglutinates with bleb like texture, quartz beads, Pelées hair, ferruginous hollow spheroids, kinked biotite, feldspars showing oscillatory zoning, native iron, olivine and many other peculiar opaques (e.g., ilmenite) which are characteristic of volcanic origin. Some of these grains are shown in figure 4. Their composition was determined using EDAX system with scanning electron microscope. The presence of particles of volcanic origin throughout the Siliceous Earth, suggests that it is volcanic ash.

The compositions of the Siliceous Earth and the Fragmental Layer (FL), the concentrations of U and Th daughter nuclides and K in a few representative samples taken from different horizons of the Siliceous Earth sections above and below the Fragmental Layer are given in table 1 and concentration profiles of U, Th, K and some elements (La, Fe, Sc, Cs, Zr, Hf, Co, Cr and Ce anomaly) in Matti ka Gol and Bariyara sections are shown in figures 5 and 6. The rare earth patterns with respect to chondrites and North American Shale Composite are shown in figure 7(a, b).

5. Discussion

5.1 *Chemical analysis*

The chemical analyses given in table 1 and the profiles given in figure 6 show that the composition of the Siliceous Earth varies significantly through the section. In Bariyara and Matti ka Gol sections, SiO_2 varies between 74.3 and 76.3%, Al_2O_3 between 0.4 and 9.1%, Fe_2O_3 between 2.1 and 2.6%, CaO between 0.7 and 2.0% and MgO between 0.4 and 0.5% (Bhargava and Pitliya 1984). The trace elements also show a similar (within a factor of 2) variation in the four samples (MG5, MG6, MG8 and MG18) studied from this section. For example, sample MG6 shows a higher concentration of several elements (lithophiles, chalcophiles and siderophiles, table 1) compared to

Table 1. *Concentration of some siderophile, lithophile, Rare earth elements, the calculated Ce anomaly, U daughter products, Th and K in various horizons of the Siliceous Earth in Matti ka Gol and Bariyara sections.* $^{214}Bi/^{234}Th$ *ratio is also given.*

	Matti ka Gol									Bariyara					
Sample no.	MG-8	MG-3	MG-6	MG-1	MG-5	MG-14	MG-2	MG-4	MG-15	BY-2	BY-1	BY-3	BY-4	BY-5	
Depth (m)	0.30	1.00	1.65	1.73	1.78	1.80	1.90	2.10	2.10	1.43	1.73	2.03	2.93	3.12	Typical
Nature		Brown-3		FL			Brown-2	Brown-1	Brown-1 (separated)		FL		Brown		error (1σ%)
Siderophile and lithophile elements															
Co (ppm)	5.3	9.7	6.0	10.1	3.5	3.3	14.6	12.4	31.7	–	2.0	–	10.2	25.1	0.2
Fe (%)	2.1	4.9	1.9	2.3	1.4	1.4	10.1	8.4	22.1	–	1.0	–	4.8	10.7	0.2
Ni (ppm)	–	53.1	–	15.2	–	–	120.9	53.1	258.9	–	3.3	–	–	–	–
Cr (ppm)	49.0	64.6	67.7	97.6	51.7	43.2	47.3	32.2	34.9	–	40.9	–	66.6	40.9	1.5
Cs (ppm)	1.0	1.1	1.2	4.1	1.2	0.9	0.9	0.8	0.6	–	1.0		1.4	1.1	3
Zr (ppm)	139.9	141.3	219.7	279.5	137.1	131.0	490.3	490.7	162.8	–	164.4	–	136.4	139.8	10
Zn (ppm)	22.5	54.7	34.0	25.1	11.4	14.7	163.7	–	411.6	–	–	–	40.4	137.1	12
Sb (ppm)	0.1	0.8	0.2	0.3	0.1	0.1	1.3	0.4	1.9	–	0.1	–	0.5	0.5	10
Ba (ppm)	63.9	163.8	90.8	186.8	53.8	55.4	138.8	77.1	66.0	–	58.5	–	110.3	99.2	15
Sc (ppm)	9.5	13.7	12.0	9.5	9.3	8.3	22.2	11.1	17.7	–	10.4	–	15.2	11.3	0.1
Hf (ppm)	3.7	3.2	7.6	7.7	3.7	3.5	2.6	2.0	1.6	–	2.6	–	2.9	1.5	1
Al (%)	–	2.96	–	4.61	–	–	1.75	1.71	0.91	–	2.75	–	–	–	–
Mg (%)	–	0.55	–	1.65	–	–	0.22	0.37	0.18	–	0.30	–	–	–	–
Na (%)	0.2	0.5	0.7	1.2	0.8	0.6	0.5	8.4	2.8	–	1.6	–	2.3	5.5	2
Rare earth elements (ppm)															
La	15.4	16.1	26.6	34.5	27.5	19.0	100.7	231.7	49.3	–	73.5	–	21.7	20.8	1
Ce	35.0	37.8	54.8	72.2	55.4	43.6	275.6	327.1	60.4	–	127.8	–	43.3	22.4	1
Nd	11.0	13.9	23.4	29.9	26.3	16.7	203.5	230.3	37.0	–	59.5	–	21.2	13.1	2
Sm	2.2	3.4	5.0	6.0	5.6	3.7	48.9	94.5	15.1	–	12.8	–	4.4	5.8	1
Eu	0.5	0.8	1.0	1.1	1.2	0.8	11.2	12.5	2.0	–	3.0	–	1.0	0.9	0.6
Gd	–	3.0	4.0	4.7	4.7	–	40.4	50.1	7.8	–	12.4	–	0.7	4.2	5
Tb	0.3	0.6	0.7	0.7	0.7	0.5	5.4	6.1	1.2	–	1.9	–	0.5	0.8	5
Yb	1.7	2.8	3.0	2.5	2.2	2.0	6.9	8.6	5.3	–	8.5	–	2.3	5.3	2
Lu	0.3	0.4	0.5	0.4	0.4	0.3	1.1	1.0	0.8	–	1.3	–	0.4	0.7	2
Ce (anomaly)	1.06	1.09	1.0	1.0	0.93	1.10	1.27	0.65	0.57	–	0.8	–	0.9	0.5	–
U, Th, K, $^{214}Bi/^{234}Th$, and Th/U ratio															
U (ppm) ^{234}Th	1.1	–	3.5	3.3	1.7	–	–	–	1.8	3.6	3.8	4.5	6.2	–	15
^{226}Ra	1.5	–	1.8	3.1	0.6	–	–	–	2.4	1.6	2.6	2.7	2.5	–	5
^{214}Bi	1.8	–	1.7	2.9	0.9	–	–	–	2.5	1.2	2.0	2.5	1.5	–	2
^{210}Pb	1.7	–	3.2	2.8	2.1	–	–	–	4.6	1.5	2.4	2.8	3.1	–	15
Th (ppm)	5.6	–	9.1	16.4	5.1	–	–	–	4.8	5.1	5.5	4.5	5.5	–	2
K (%)	0.3	–	0.2	1.1	0.1	–	–	–	0.2	0.2	0.2	0.2	0.2	–	2
Th/U	3.6	–	5.6	5.0	6.1	–	–	–	1.9	4.3	3.2	2.2	3.9	–	–
$^{214}Bi/^{234}Th$	1.6	–	0.5	0.9	0.5	–	–	–	1.4	0.3	0.5	0.5	0.2	–	–

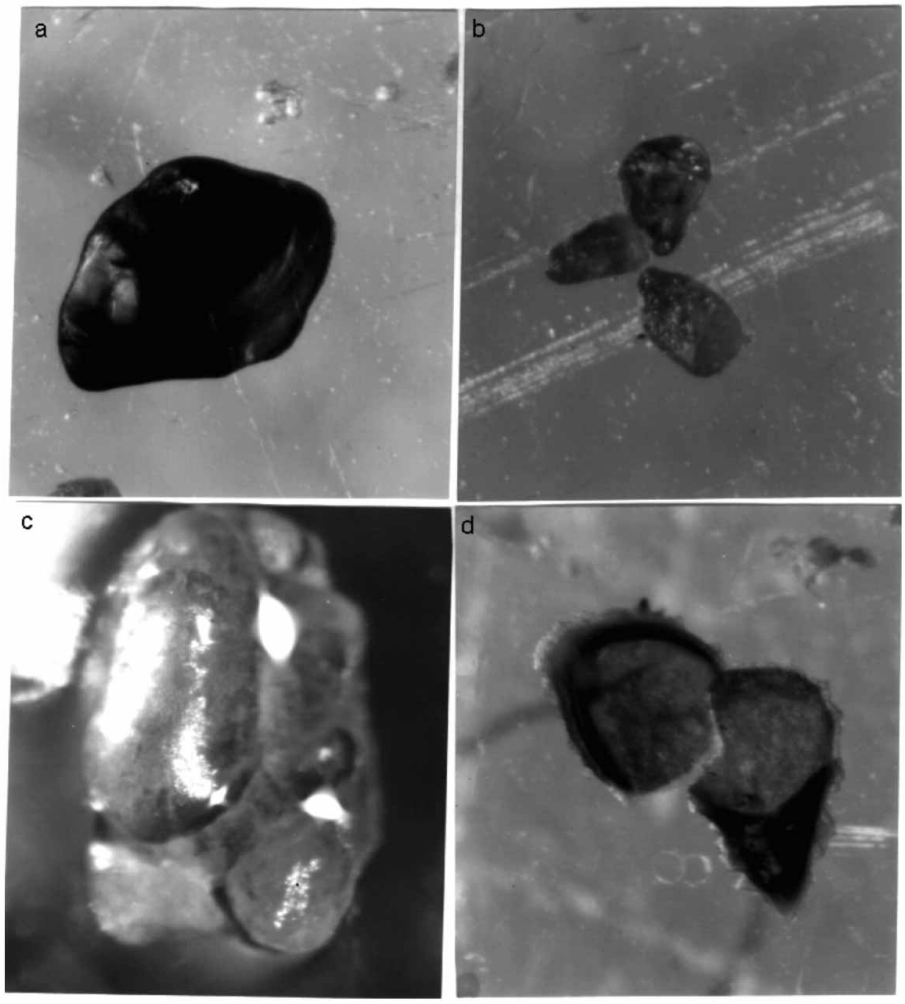

Figure 4. Photomicrographs of some typical particles seen in the loose fragmental layer from Matti ka Gol. Figure 4**(a, b)** glass shards, **(a)** glass with concoidal features **(c)** quartz agglutinate, **(d)** a thin metallic hollow sphere, broken in to two during handling.

the other three samples (MG5, MG8 and MG18). These results indicate that chemically different components are present at different horizons of the Siliceous Earth. Depth profiles of most elements (figure 6) do not show any trend, which would be expected if weathering, leaching or remobilization had played a significant role in the distribution of elements within the section. Therefore, the Siliceous Earth seems to represent a sequential deposit of material having different concentrations of various elements.

The loose fragmental layer (FL) at Matti ka Gol (MG11) shows enrichment of certain elements (Hf, Cr, Cs) whereas the brown bands (MG4, 2 and 3) are enriched in REE, Fe, Sc, Zr and chalcophiles (Zn and Sb), as compared to the average composition of the Siliceous Earth. MG15, the rusty separate of MG4, shows extremely high concentration of several elements (Co, Fe, Ni, Zn, Sb). High concentration of Zr in MG-2 and MG-4 samples compared to rest of the samples could be due to the presence of zircons.

We now compare their composition quantitatively with respect to the composition of the Siliceous Earth. The brown limonitic bands are significantly enriched in Fe, Ni and Zr and, two of them also in La and Sc, although the enrichment is not identical in all of them. The lithophile elements Hf, Zr, Cs, U, Th, K and Cr are significantly higher in FL (Hf = 7.7 ppm, Zr = 280 ppm, Cs = 4.1 ppm, U = 2.9 ppm, Th = 16.4 ppm, K = 1.1%, Cr = 97.6 ppm) compared to the general levels found in the Siliceous Earth, excluding the brown layers (Hf = 3.6 ppm, Zr = 13.1 ppm, Cs = 1.1 ppm, U = 0.9 to 2.5 ppm, Th = 4.5 to 9.1 ppm, K = 0.1 to 0.3%, Cr = 47.5 ppm). The enhancement factors for the concentration of various elements in the fragmental layer (MG-1) above the general levels are (Zr = 21.3, K = 11.0, Hf = 91 and Th, U, Co, Cr, Ba and Sb about 3). The

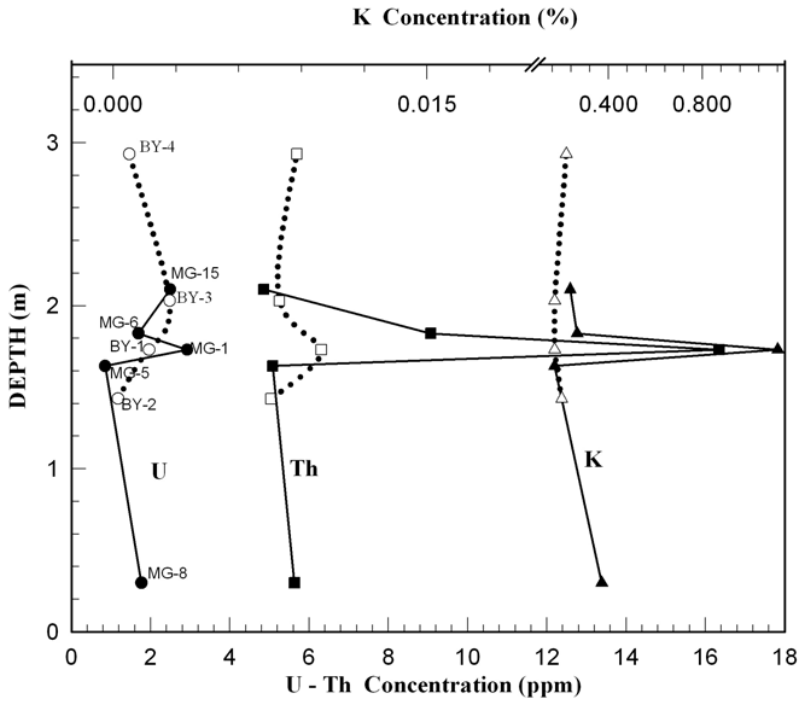

Figure 5. U–Th–K depth profile (Matti ka Gol (closed symbol) and Bariyara (open symbol)).

concentration of Fe, Co, Sc, La are also marginally higher (>1.5 times). The high concentration of these elements can be attributed to acidic volcanism. Fe, Co, Ba, Zr, Sb and Sc are also enriched in the limonitic layers but to a lesser degree. It is clear from figures 5–10 that although the fragmental layers at Matti ka Gol (MG1) and at Bariyara (BY1) have a similar appearance, their chemical composition is not identical. The enrichments of many elements e.g., U, Th, K, Cs, Hf, Cr are not as marked in BY1 as in MG1, whereas REE concentrations are much higher in BY1 compared to MG1, although the patterns are similar (figure 7). The REE concentration in Siliceous Earth remain within a factor of 2 and $(La/Lu)_{CN}$ varies between 5.3 and 7.1 indicating a similar LREE enrichment among the four samples mentioned above.

La/Th and Th/Yb ratios are distinguishably different in basaltic, granitic and shaly components (Wang *et al* 1986) and can be used to identify the provenance of different strata of the Siliceous Earth. These ratios (figure 8) vary significantly in the fragmental layer and limonitic layers compared to the other strata of the Siliceous Earth where they remain within a narrow range (La/Th = 2.6 to 3.7; Th/Yb = 2.8 to 3.5). The Th/Yb ratio for fragmental layer (MG1) shows a small peak (Th/Yb = 5.3) whereas above and below FL the value is ∼3. La/Th and Th/Yb ratios of 2.6 and 5.3 respectively for FL are typical of shales and reflect a change in provenance when this layer was deposited.

Correlation diagrams for some elements are given in figure 9. It seems that Fe, Ni and Co correlate with each other (as well as with Sb, not shown in the figure) whereas Cr and Ni are inversely correlated. The limonitic layers not only have a higher concentration of Fe but also of chalcophiles like Zn and Sb as well as REE (table 1). Enhancement of chalcophiles in marine as well as continental sections have been observed in many K/T sections all over the world (Schmitz 1992). In the K/T sections, the enrichment of chalcophiles and their covariation with Fe has been attributed to weathering of goethite, pyrite, etc. During these processes, ferric hydroxide acts as a scavenger, enriching a variety of chemically diverse elements including REEs. By analogy, similar processes may have operated in the source regions resulting in high concentrations of REEs and other elements as well as high La/Th and low Th/Yb (figure 8) in the limonitic layers.

5.2 *Concentration of U, Th daughters and origin of excess* ^{210}Pb

The data given in table 1 show that all the ^{238}U daughter nuclides are not in secular equilibrium. ^{214}Bi actually reflects the concentration of ^{226}Ra measured directly (at 186.1 keV) and via ^{214}Bi (609.3 keV) and the small differences in the values determined based on the two energies may be due to slight interference in radium energy peak. The difference between ^{234}Th, ^{214}Bi and ^{210}Pb (table 1)

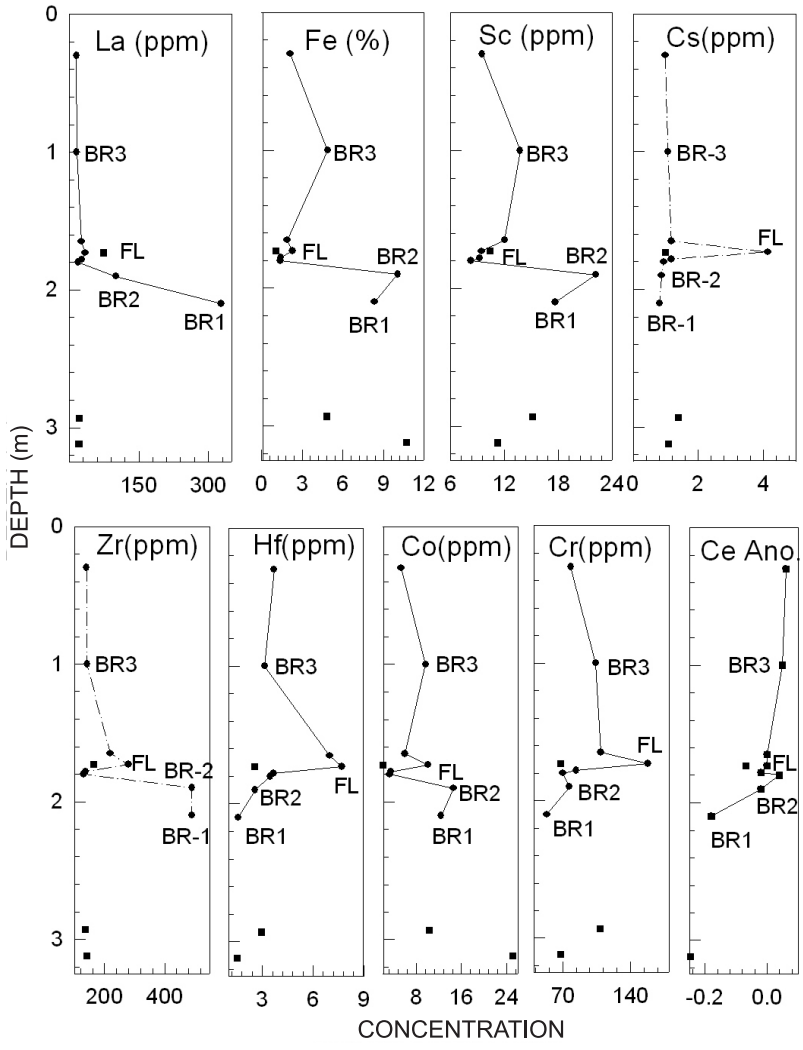

Figure 6. Vertical profiles of La, Fe, Sc, Cs, Zr, Hf, Co, Cr in Matti ka Gol (circles) and Bariyara (squares) sections. The cerium anomaly is also shown.

are, however, significant. $^{214}Bi/^{234}Th$ ratios (figure 10) show a significant departure from the equilibrium value of 1 in many samples. In Bariyara samples the ratio is about 0.4 whereas the FL and its adjacent samples in Matti ka Gol have values close to 0.5. These results suggest loss of ^{226}Ra or other ^{234}Th daughters in these samples. We obtain, uncorrected for disequilibrium, values of U = 2.9 ppm and Th = 14.6 ppm which are much higher in the fragmental layer compared to the Siliceous Earth (U = 0.8–1.8 ppm, Th = 4.7–9.4 ppm). This can also be seen from the $^{228}Th/^{226}Ra$ (= Th/U) profiles shown in figure 10. In FL, the concentration of K is calculated to be 1.12% compared to the value of 0.1 to 0.3% in the Siliceous Earth. These high values reflect the acidic character of the fragmental layer.

In many samples (table 1), the ^{210}Pb activity shows an excess over its parent ^{214}Pb (^{222}Rn). One of the ways in which this excess can arise is by absorption of ^{210}Pb from rainwater that contains high activity of ^{210}Pb arising from diffusion of radon from the ground (Bhandari 1965). The ^{210}Pb excess is the highest in the limonitic part of the lowest limonitic layer (MG15), indicating that the Siliceous Earth significantly absorbs it only when a suitable chemically reactive matrix is present.

5.3 *Origin of the Siliceous Earth*

Material having physical and chemical characteristics similar to that of the Siliceous Earth can be produced in nature in two possible ways. Shells or frustules of diatoms can produce diatomite, both marine and non-marine. Alternatively, in volcanic regions, opaline silica or siliceous sinter can be produced by secretion of silica by algae in the vicinity of hot springs and also form a siliceous deposit/geyserite due to evaporation. It is also possible that volcanism provides the primary source of

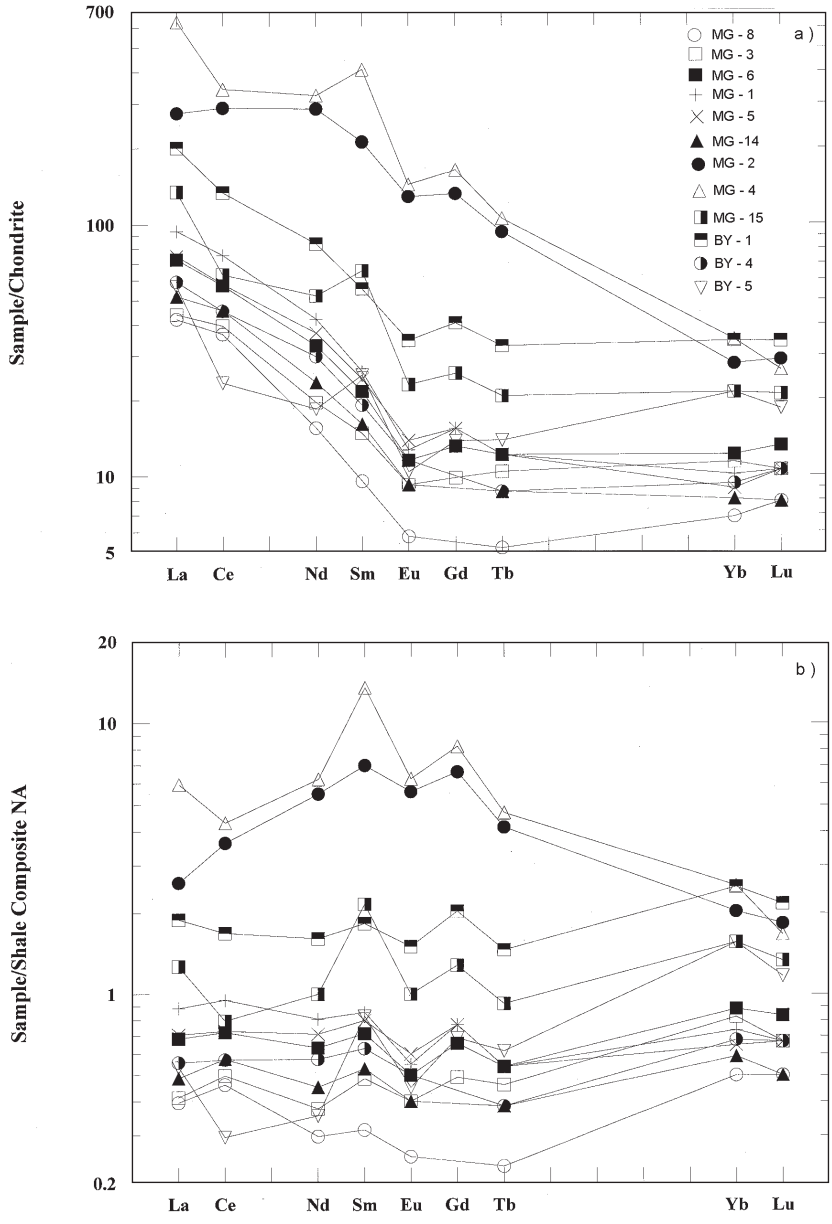

Figure 7. The rare earth element pattern in some Matti ka Gol and Bariyara samples. **(a)** normalised to chondrites **(b)** normalised to North American Shale Composite.

silica necessary for the growth of diatoms, which eventually give rise to diatomite.

In view of the presence of the particles characteristic of volcanic origin throughout the Siliceous Earth, there is no doubt that a volcanic component is present. The concentration of U (^{226}Ra) and Th (^{228}Th $\equiv$ ^{208}Tl) in Siliceous Earth is also higher than that expected in a marine diatomite. The seawater does not contain much thorium and ^{208}Tl/^{226}Ra in diatomite is expected to be extremely low ($\ll 1$). The value of ^{208}Tl/^{226}Ra = 1.9 to 6.0 observed in various horizons support a non-marine origin of the Siliceous Earth. Microscopic examination as well as maceral treatment did not reveal the presence of any shells or frustules of diatoms expected in diatomite. The enrichment of lithophile elements (Zr, K, Hf, Th, U, Cr, Ba, Sb, Sc and La) discussed above suggests that the Siliceous Earth is not a diatomite but originated by acidic volcanism.

5.4 *Stratigraphic, palaeontological and geochronological controls*

In order to understand the formation of the Siliceous Earth and origin of peculiar grains observed at some horizons, it is necessary to have a geochronological framework. Pareek (1981) has correlated the Fatehgarh sandstone, over which the Siliceous Earth is located, with Abur limestone of

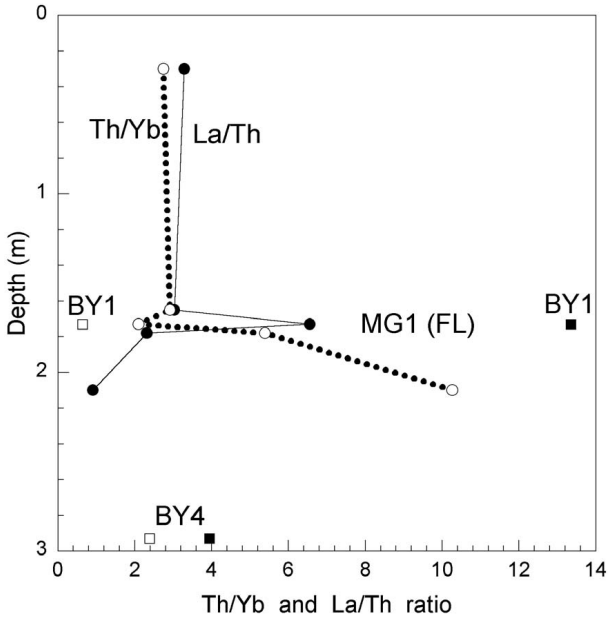

Figure 8. La/Th (filled symbols, solid line) and Th/Yb (open symbols, broken line) ratios variation with depth in the Matti ka Gol (circles) and Bariyara (squares) sections. The MG-1 (FL) samples shows a high value of Th/Yb ratio, similar to shales.

Jaisalmer Basin, which contains ammonoid fossils of Cretaceous age. Mishra *et al* (1993) assigned a Palaeocene age to this formation on the basis of regional stratigraphic correlations. The recent finding of microvertebrates of Late Cretaceous age in Fatehgarh Formation (Mathur *et al* 2005) establishes the age of the this formation as Late Cretaceous.

Palynological investigation of interbedded shales in lignites of Akli Formation which unconformably overlies Fatehgarh Sandstone and Siliceous Earth carried out by Tripathi *et al* (2003) shows the dominance of *Dandotiaspora, Lycopodiumsporites, Palmaepollenites, Spinizonocolpites, Palmidites, Psilastephanocolporites* and *Granustephanocolpites*, most of which are index fossils of Late Palaeocene. The assemblage lacks the early Eocene marker palynotaxa like *Tricolporopollis matanomadhensis, Meliapollis ramanujamii, M. pachydermis, M. simplex, Umbelliferroipollenites ovatus* and *Pellicieroipollis langenheimii*. The observed palynofloral assemblage thus indicates Middle to Late Palaeocene age to the sequence unconformably overlying Siliceous Earth.

It may be noted that a sodalite intrusive covering an area of over 200 km^2 occurs in the vicinity at Sarnu–Dandali (N24°41.550′; E71°55.279′). This intrusive body is pale pinkish in colour and is composed of sodic feldspar with minor mafic minerals. Dark green nephelinite dykes have intruded it. Carbonatite dykes and andesitic dykes also occur in the area. These intrusives are emplaced in the Malani Rhyolite basement rocks. A firm datum, based on geochronological ages of the alkaline and

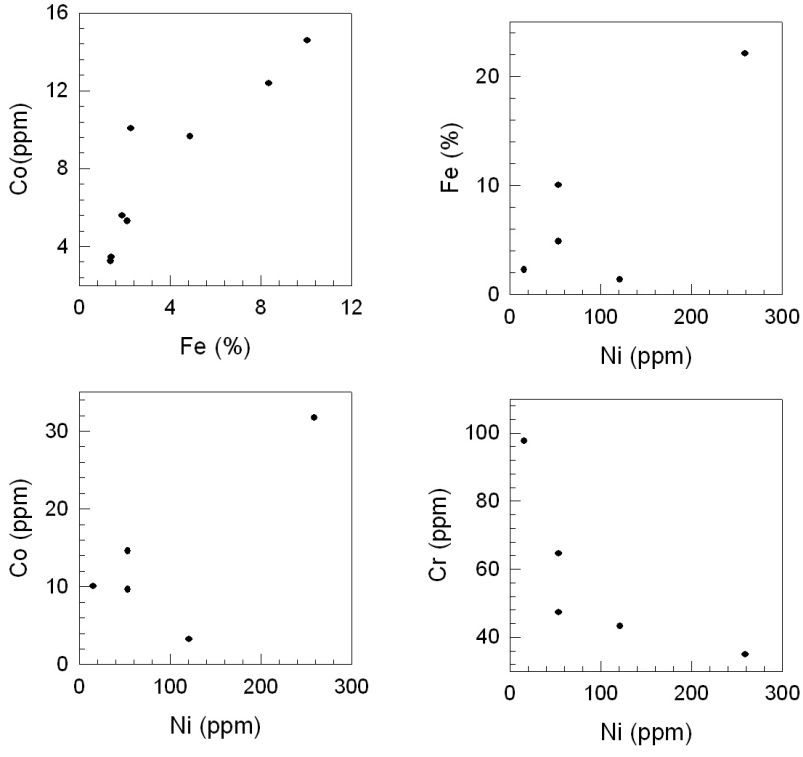

Figure 9. The correlation diagram of Fe, Co, Cr and Ni in the Siliceous Earth of Matti ka Gol.

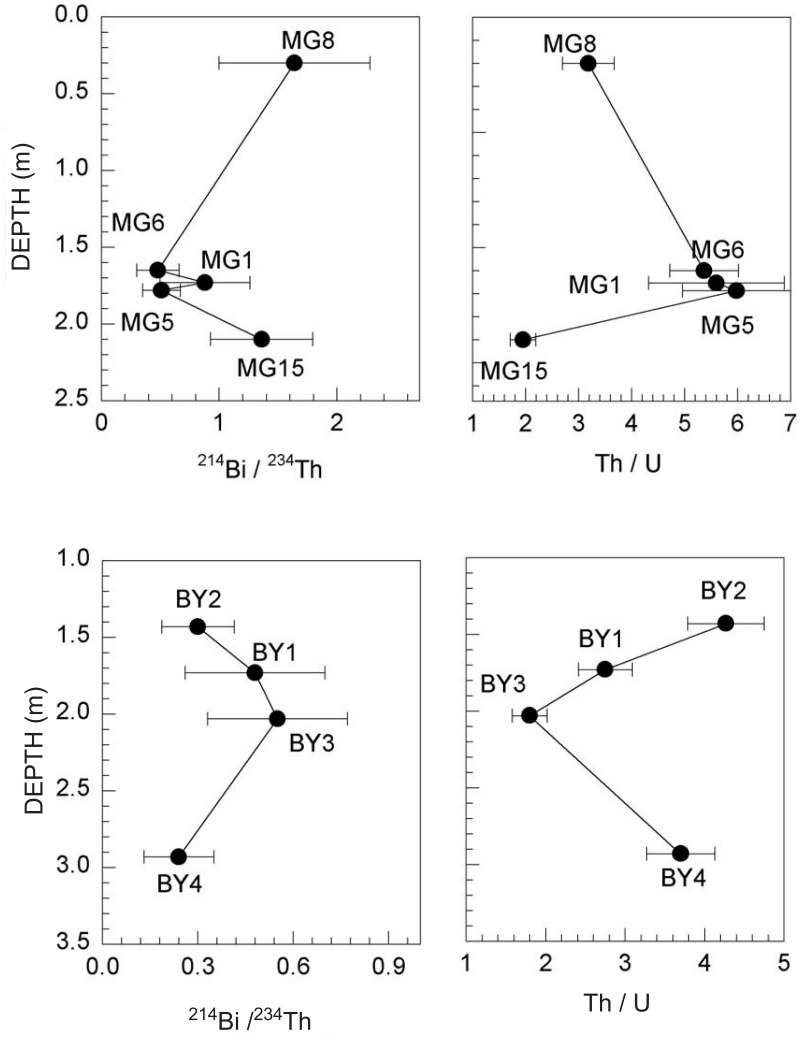

Figure 10. ^{214}Bi/^{234}Th and Th/U profiles in the Siliceous Earth at Matti ka Gol (MG) and Bariyara (BY).

paralkaline rocks exposed at Sarnu–Dandali, which are correlated with Fatehgarh formation has been obtained. These igneous rocks have been dated radiometrically by ^{40}Ar–^{39}Ar method (Basu *et al* 1993; Venkatesan 1990; Rathore 1995). They show ages of 67 ± 2.1 Ma and 64.9 ± 2 Ma, and are probably related to the Deccan volcanism which was active during 68 to 61 Ma as indicated by the ages of Anjar basalt flow sequence in the nearby Kutchch region (Bhandari *et al* 1995; Venkatesan *et al* 1996, Shukla *et al* 2002). Basu *et al* (1993) have also dated biotite grains from the Sarnu–Dandali intrusive alkali pyroxenites and got a mean age of 68.57 ± 0.08 Ma while intermediate basic rocks (andesites) dated by Venkatesan (1990) show age as 64.9 Ma. The Sarnu–Dandali intrusives therefore represent an episode of alkaline/subalkaline magmatism close to the Cretaceous–Tertiary boundary which is dated by Izett *et al* (1991) at 65.2 ± 0.1 Ma. However, it is difficult to establish any field relationship of the siliceous earth with any of the nearby magmatic events except to say that our chemical and mineralogical studies indicate that siliceous earth had a volcanic origin.

In summary, the chronological constraints described above show that the Siliceous Earth of Barmer basin was accumulated over a short span of time during Late Cretaceous to Palaeocene.

5.5 *Relevance to the K/T boundary event*

As discussed above, the geochronological and palynological data, taken together, thus suggest that the loose fragmental layer under discussion formed close to the K/T boundary. At the K/T boundary, one large crater at Chicxulub is well documented (Sharpton *et al* 1996). Two more craters in the vicinity of western India have been proposed but no evidence has so far been found. Chatterjee and Rudra (1996) have proposed the formation of a giant (600 km diameter) Shiva Crater at the

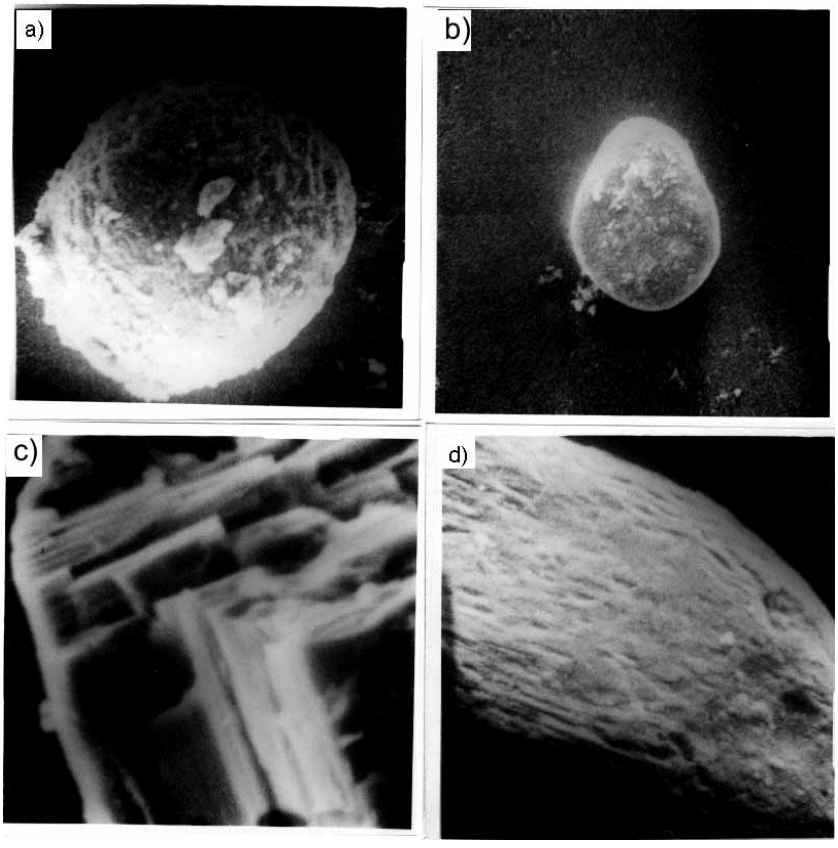

Figure 11. Micrometeorite ablation products such as spheroids and tear drop **(a, b)** and grains showing skeletal structure **(c)**. A magnified view of the spheroid **(a)** is shown in **(d)**.

India–Seychelles border that gave rise to the Carlsberg ridge. Negi *et al* (1992) have proposed formation of a smaller crater near Bombay at about the same time. Therefore, a search for impact debris was undertaken in the Siliceous Earth because it has uniform mineral composition that is distinctly different and easily distinguishable from impact ejecta. We did not find any grains that can be suspected as impact ejecta at Matti ka Gol. At Bariyara, however microthin patches containing particles that include glasses with high nickel content, a few sanidine spherules and possibly magnesioferrite crystals with skeletal growth texture and, in rare cases, lamellae were found. Some of these grains are shown in figure 11. The chemical analysis of glasses of size up to 0.1 mm shows some nickel rich opaques (0.5 to 2% Ni) (figure 12a, b). The Ni is not homogeneously distributed throughout the glasses but is present only in the surficial regions as shown by the energy dispersive X-ray spectra determined using a scanning electron microscope (figure 12). Nickel is abundantly present in various types of meteorites but occurs in very low concentration in terrestrial rocks except in primary mantle-derived mafic and ultra mafic magmas, where its concentration is high. The similarity of other particles (sanidine spheres, skeletal magnesioferrites, etc.) to those found in Chicxulub ejecta debris in the K/T boundary deposits at many sites in the Pacific (e.g., see Smit and Klaver 1981; Zhou *et al* 1991) may indicate an impact, but shocked quartz, considered to be a definite evidence of impact (Bohor 1990) was not found.

6. Summary

Based on the nature of particles and trace element systematics (Th/U and enrichment of lithophile elements like Zr, K, Hf, Cs, etc.) it is concluded that the Siliceous Earth found in the Barmer basin of Rajasthan is a volcanic ash. Microscopic examination did not reveal the presence of shells or frustules of diatoms indicating that it is not of marine diatomitic origin. A peculiar layer, a few centimetres thick, found within the section, is highly enriched in some rare earth elements. There is some evidence of Ni bearing vesicular glasses, sanidine spherules, magnesioferrite crystals, soot, etc. identified in small patches that may have origin in impact related processes, requiring further study.

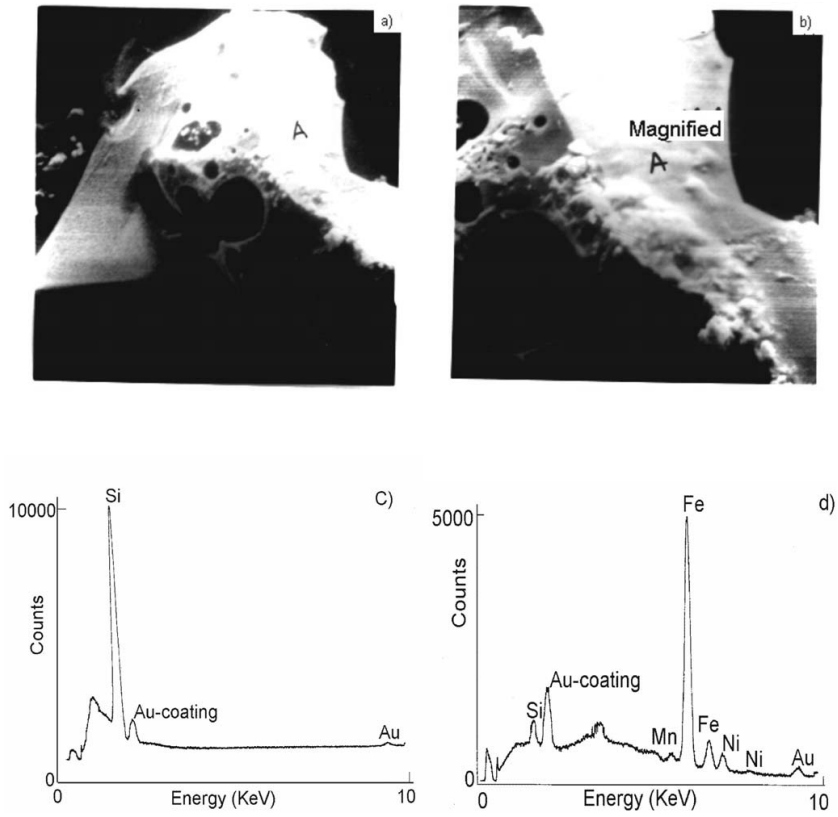

Figure 12. Scanning electron photomicrograph of **(a)** a vesicular glass **(b)** and its nickel rich region. The X-ray spectra of the two regions **(c and d)** show Si and Ni rich regions. Nickel is associated with iron and small amounts of silicon and manganese. The gold peak is due to gold coating of the section.

Acknowledgements

We thank Mr. V G Shah for technical assistance which made SEM studies possible. We were benefited by discussions with Drs. S Krishnaswami, M M Sarin (PRL), D J Corbishley, R G McElroy and S M Saxena (Shell Oil). Research grant provided by Shell India Production Development BV and Associateship of Physical Research Laboratory to MSS is gratefully acknowledged. Constructive suggestions by Dr. Hetu Sheth as one of the reviewers of this paper helped in the improvement of this paper.

References

Basu A R, Paul R R, Das Gupta D K, Teichmann F and Poreda R J 1993 Early and late Alkali Igneous Pulses and a High $-^3$He Plume for the Deccan Flood Basalts, *Science* **261** 902–906.

Bhandari N 1965 Studies of some physical processes occurring in the atmosphere based on radionuclides of natural and artificial origin. Ph.D. Thesis, Bombay University, p. 164.

Bhandari N, Shukla P N, Ghevariya Z G and Sundaram S M 1995 Impact did not trigger Deccan volcanism: Evidence from Anjar K/T boundary intertrappean sediments; *Geophys. Res. Lett.* **22** 433–436.

Bhargava K D and Pitliya N M 1984 Siliceous Earth of Barmer District, Rajasthan, Unpublished report, Department of Mines and Geology, Rajasthan, p. 15.

Bohor B F 1990 Shocked quartz and more; impact signatures in Cretaceous/Tertiary boundary clays; *Geol. Soc. Am. Paper* **247** 335–342.

Chatterjee S and Rudra D K 1996 KT events in India: impact, rifting, volcanism and dinosaur extinction. Gondwana Dinosaurs: Phylogeny and Palaeobiogeography; (eds) Molnar R E and Novas F E, Mem. Queensland Mus., Australia, Pp. 103–146.

Das Gupta S K 1975 A revision of the Mesozoic–Tertiary stratigraphy of the Jaisalmer basin, Rajasthan; *Ind. J. Earth Sci.* **2** 77–94.

Izett G A, Dalrymple G B and Snee L W 1991 ^{40}Ar–^{39}Ar age of Cretaceous–Tertiary boundary tektites from Haiti; *Science* **252** 1539–1542.

Mathur S C, Mathur S K and Loyal R S 2005 A new report of late Cretaceous microvertebrates from Fatehgarh Formation *J. Geol. Soc. India* (in Press).

Mishra P C, Singh N P, Sharma D C, Upadhyay H, Kakroo A K and Saini M L 1993 Lithostratigraphy of western Rajasthan; ONGC Report, Unpublished, p. 125.

Nahar N M, Sisodia M S and Purohit M M 1997 Siliceous Earth for solar thermal energy storage; *J. Solar Energy Soc. Ind.* **7** 103–106.

Negi J G, Agarwal P K, Pande O P and Singh A P 1992 A possible K–T boundary bolide impact site offshore near Bombay and triggering of rapid Deccan volcanism; *Phys. Earth Planet. Inter.* **206** 341–350.

Pareek H S 1981 Basin configuration and sedimentary stratigraphy of western Rajasthan; *J. Geol. Soc. India* **22** 517–527.

Rathore S S 1995 Geochronological studies of Malani volcanics and associated igneous rocks of southwest Rajasthan, India: Implication to crustal evolution, Ph.D. Thesis, M.S. University, Baroda, p. 175.

Schmitz B 1992 Chalcophile elements and Ir in continental Cretaceous–Tertiary boundary clays from the western interior of the USA; *Geochim. Cosmochim. Acta* **56** 1695–1703.

Sharpton V L, Marine L, Carney J L, Lee S, Ryder G, Schuraytz V C, Sikora P and Spudis P D 1996 A model of the Chicxulub impact basin based on evaluation of geophysical data, Well logs and drill core samples; *Geol. Soc. Am. Spec. Pap.* **307** 55–74.

Sisodia M S and Singh U K 2000 Depositional environment and hydrocarbon prospects of the Barmer Basin, Rajasthan, India; *Nafta* **51** 309–326.

Smit J and Klaver G 1981 Sanidine spherules at the Cretaceous–Tertiary boundary indicate a large impact event; *Nature* **292** 47–49.

Tripathi S K M, Singh U K and Sisodia M S 2003 Palynological investigation and environmental interpretation of Late Palaeocene sediments from Barmer Basin, Western Rajasthan, India; *Palaeobotanist* **52** 87–95.

Venkatesan T R 1990 Ar–Ar studies of Malani complex in Rajasthan, India: Evidences for different magmatic episodes; *J. Geol. Soc. Australia* **27** 106.

Venkatesan T R, Pande K and Ghevariya Z G 1996 $^{40}Ar/^{39}Ar$ ages of Anjar Traps, western Deccan Province (India) and its relation to Cretaceous–Tertiary boundary events; *Curr. Sci.* **70** 990–996.

Wang Y L, Liu Y G and Schmitt R A 1986 Rare Earth element geochemistry of South Atlantic deep-sea sediments; Ce-anomaly change at $\sim$ 54 Ma; *Geochim. Cosmochim. Acta* **50** 1337–1355.

Zhou L, Kyte F T and Bohor B F 1991 The Cretaceous/Tertiary boundary of DSDP site 596, South Pacific; *Geology* **19** 694–697.

MS received 27 January 2004; accepted 5 January 2005